PII: S0032-3861(97)10141-0

Polymer Vol. 39 No. 19, pp. 4621–4629, 1998

0032-3861/98/$19.00+0.00

Structure formation in polymer solutions

H. Berghmans*, R. De Cooman, J. De Rudder and R. Koningsveld
Katholieke Universiteit Leuven, Laboratory for Polymer Research, Celestijnenlaan, 200F, B-3001 Heverlee, Belgium
(Received 17 July 1997; revised 17 September 1997; accepted 19 September 1997)

The formation of porous materials by thermally induced phase separation is discussed and two basic mechanisms are presented: interference of a liquid–liquid demixing with a glass transition and/or crystallization. The possibility of formation of porous 'composite' fibres using a blend of two non-compatible polymers is illustrated. The formation of these fibres during extrusion leads to a fibrillar morphology with the porosity oriented along the fibre axis. The formation of porous syndiotactic polystyrene with different degrees of supramolecular organization is discussed. The transformation on heating of the initially amorphous, glassy material into the γ-phase and then into the β-phase makes it possible to maintain the demixed situation up to temperatures far above the Θ-temperature of this polymer–solvent system. © 1998 Elsevier Science Ltd. All rights reserved.

(Keywords: liquid–liquid phase separation; porous composite fibres; porous syndiotactic polystyrene)

INTRODUCTION

Thermally induced phase separation is a very easy technique for the production of porous materials like membranes, porous fibres, etc. The basic principle is the interference between a liquid–liquid demixing (L–L demixing) process in a polymer solution and a solidification process by vitrification or crystallization. After elimination of the solvent, a porous material is obtained[1–3]. The basic principles and experimental illustrations have been discussed in previous papers[4,5,1,2]. They will be summarized in the following paragraphs. Volume fractions (ϕ) should be used in these discussions and this is done so in the schematized diagrams. But for practical reasons, experimental data are generally presented as weight fractions (w).

Porous materials by L–L demixing and vitrification

Such a combination of thermal transitions can best be understood through the corresponding temperature–concentration diagram, as illustrated in *Figure 1* for a solution of a non-crystallizable polymer. Solidification proceeds by vitrification only, and the system shows upper critical solution temperature behaviour (UCST). The polymer is supposed to be monodisperse so that the binodal coincides with the cloud point curve. A solution with composition X will demix in two coexisting solutions with composition ϕ_2' and ϕ_2'' when cooled from T_1 to T_2. This demixing will proceed when cooling is continued and the concentrations of the coexisting phases ϕ_2' and ϕ_2'' will follow the binodal on both sides of X until T_g^d is reached and the concentrated phase (ϕ_2^d) vitrifies. The composition of this concentrated phase will not depend on the initial overall concentration. Therefore T_g will remain constant in the concentration range $0 < \phi_2 < \phi_2^d$. The dilute phase will be a very dilute polymer solution or even almost pure solvent. In the initial stages of the demixing a phase-separated situation composed of many small domains of high and low polymer content will exist. At low overall polymer concentration, droplets of the concentrate will be dispersed in a dilute matrix. Phase inversion will take place at high polymer content, resulting in a concentrated matrix with dispersed droplets of low polymer concentration. At intermediate concentrations, interesting bicontinuous structures can be generated. Such a multi-domain, two-phase system has to evolve towards its final equilibrium situation: a system composed of only two layers with different polymer content. But this will almost never be realized when polymers are involved because of the high viscosities involved. When this non-equilibrium situation is frozen by vitrification and the solvent is eliminated, a porous material is obtained. The morphology of such a porous material will not only be the result of the polymer–solvent phase behaviour, but will depend to a large extent on the experimental conditions and the characteristics of the system.

The time that is given to the system before it is frozen by vitrification of the concentrated domains is important. In a dynamic process, the rate of cooling will be important as the size of the domains will increase with decreasing cooling rate[6]. The introduction of an isothermal annealing period at $T > T_g^d$ will have the same effect.

The characteristics of the system itself will also affect the final result. This includes the molar mass of the polymer and its distribution, influencing the viscosity of the polymer-rich phase, the properties of the solvent and the diffusion characteristics of the demixed system. The elimination of the solvent after the formation of the structure can also affect the final morphology. The vitrified domains can contain a weight fraction of solvent up to 0.25, and this is generally eliminated by extraction and/or drying at elevated temperatures. Up to now it has not been possible to evaluate experimentally the influence of this last parameter and the morphologies that will be presented will be the result of the combination of all these parameters.

While the situation is rather well understood at $T > T_g^d$, questions can still be asked about the evolution of the demixed and frozen system when it is cooled to and annealed at $T_{an} < T_g^d$. At this temperature, a demixed, vitrified system with the composition of the concentrated

---

* To whom correspondence should be addressed

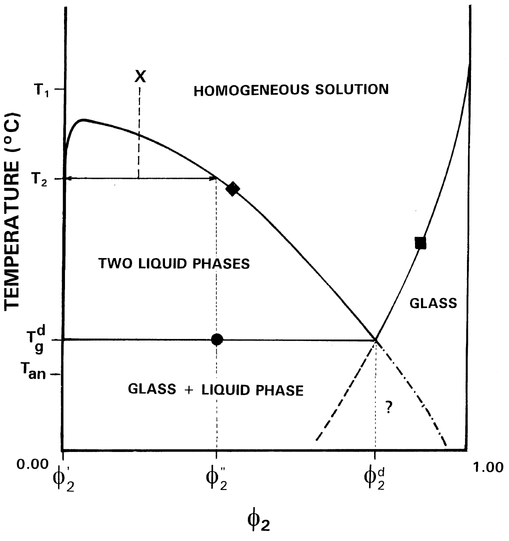

Figure 1 Schematic representation of the interference between a liquid–liquid demixing and a glass transition. – ◆ –, binodal; – ■ –, T_g–concentration relation; – • –, T_g–concentration under the binodal; – · –, expected demixing curve in the glassy state at $T < T_g^d$ and $\phi_2 > \phi_2^d$; - - -, expected glass transition–concentration curve at $T < T_g^d$ and $\phi_2 < \phi_2^d$

phase equal to ϕ_2^d, will be glassy as it is situated below the expected T_g–concentration curve (- - -). But the system will not be in thermodynamic equilibrium and is supposed to evolve towards the expected L–L demixing curve (- · - · -). Therefore two opposing effects will be operative: the important reduction of molecular mobility in the glassy state limiting any further evolution of the system, and the thermodynamic driving force towards the equilibrium demixed state. The same problem is encountered when a solution with $\phi_2 > \phi_2^d$ is cooled. On cooling this solution will vitrify when the glass transition–concentration curve is crossed (■) and form a homogeneous glassy phase. When the sample is cooled to a temperature situated below the expected demixing line (- · - · -), L–L demixing should take place. But this process will also be hindered by the limitations in molecular diffusion in the glassy state. Up to now, no firm experimental evidence has been obtained to come to any valid conclusion, and therefore a question mark has been placed in the corresponding temperature–concentration field.

Porous materials by L–L demixing and crystallization

The situation is different when freezing proceeds by crystallization from the concentrated phase[2]. The curve representing the concentration dependence of the melting temperature intersects with the binodal and a three-phase equilibrium is generated. This leads to an non-variant melting point in the concentration domain under the demixing curve. The presence of a polymer raises additional problems. Polymer crystallization proceeds at a certain degree of undercooling so that the interference between demixing and crystallization will take place at the temperature and concentration that correspond to this intersection point between the crystallization line (concentration dependence of the crystallization temperature) and the binodal. Melting proceeds at a higher temperature. Such a situation is illustrated in *Figure 2* for a binary polymer–solvent system. An increase of T_m with decreasing overall polymer content can be observed in the concentration range under the miscibility gap when dealing with a polydisperse polymer[2].

These different thermal transitions can compete with each other when crystallization and L–L demixing take place in the same temperature domain. This situation is realized in the system poly(2,6-dimethylphenylene oxide) (PPO)/cyclohexanol[6,7]. Crystallization sets in only a few degrees above the demixing temperature. Slow cooling will result in crystallization only, and no interesting porous structure will be obtained. On increasing the cooling rate, crystallization will interfere with the L–L demixing and crystalline porous materials will be obtained. At a high enough cooling rate, demixing interferes with vitrification only, leading to an amorphous, porous material. This last demixing process has been used for the production of hollow, porous fibres[6,7].

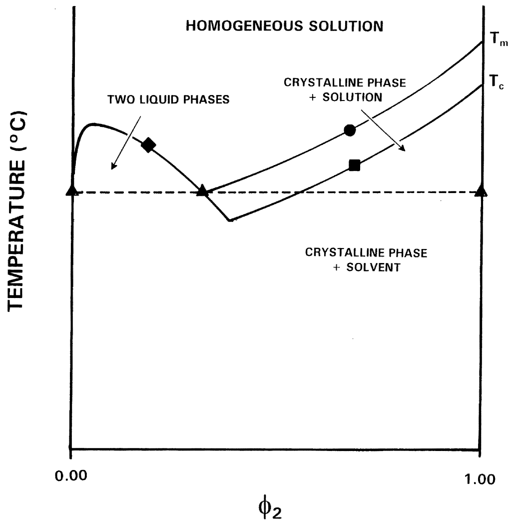

Figure 2 Schematic representation of the interference between a liquid–liquid demixing and a melting and crystallization process. – ◆ –, binodal; – ■ –, T_c–concentration relation; – • –, T_m–concentration under the binodal; ▲, invariant three-phase equilibrium

EXPERIMENTAL

Polymers

Poly(methyl methacrylate) (PMMA) and poly(ethyl methacrylate) (PEMA) were prepared by radical polymerization in bulk, with AIBN as the initiator. The polymers are atactic and their weight and number average molecular masses in kg/mol are: (1) PMMA, $M_w = 250$, $M_n = 156$; (2) PEMA, $M_w = 210$, $M_n = 100$.

Syndiotactic polystyrene was obtained from Dow Chemical. The number- and mass-average molecular masses, determined by g.p.c. in 1,2,4-trichlorobenzene, are 143 and 429 kg/mol.

Dynamic scanning calorimetry

A Perkin-Elmer DSC-7 was used to study thermal transitions at 5°C/min. The polymer weight fraction, w_2, is used to express the polymer concentration: (1) liquid-liquid demixing (the temperature at the onset of the demixing exotherm is taken as the demixing temperature); (2) crystallization (the temperature at the onset of the crystallization exotherm is taken as the crystallization temperature); (3) melting (in polymer–solvent systems, the temperature at the end of the melting endotherm is taken as the melting temperature).

Fourier transform infrared spectroscopy

A Perkin-Elmer FTIR 2000 was used. The solution is placed between NaCl windows in a cell with the necessary temperature control.

Wide-angle X-ray scattering

A Rigaku Rotaflex 200B rotating anode spectrometer equipped with a Bragg-Brantano focussing diffractometer and an intensity counter was used operating at 40 kV and 100 mA, generating Ni-filtered Cu Kα radiation.

Electron microscopic observations

Electron microscopic observations were made with a Cambridge Stereoscan 200C.

Liquid–liquid demixing

The temperature at which the first traces of opalescence are observed is taken as the demixing temperature. A very good agreement is obtained with the demixing temperature determined by calorimetric observations.

Extrusion

The experimental conditions for extrusion were deduced from the temperature–concentration diagram of the system. A mini twin-screw extruder with a spin hole of 1 mm was used. This extruder was supplied by professor H. Meijer of the TU Eindhoven. The polymer–solvent systems were prepared at 85°C and extrusion was performed at this temperature. The extrudate was cooled to room temperature and simultaneously stretched by hand. Most of the solvent evaporated during this treatment and the remainder was eliminated by prolonged drying under vacuum. The samples were cut parallel to the fiber axis and their morphology was investigated by scanning electron microscopy.

DEMIXING IN SOLUTIONS OF POLYMER BLENDS

Production of porous 'composite' fibres

Porous fibres in which porosity extends as micrometer channels along the fibre axis can be obtained when demixing is combined with the extrusion of the initially homogeneous solution[8]. This technique leads to the formation of interesting 'composite' fibres by extruding solutions of two chemically different, mutually incompatible polymers in a common Θ-solvent[9]. Fibres are formed with an internal fibrillar texture oriented along the fibre axis and these fibrils are separated by channels with a diameter in the micrometer range. The fibrils are mainly composed of the polymer that demixes at the highest temperature and that is present in excess, while the polymer with the lowest demixing temperature is deposited on the surface of these fibrils on further cooling. An example of such a morphology is represented in *Figure 3a*. The fibres were obtained by extrusion of a solution of poly(methyl methacrylate) (PMMA) and poly(ethyl methacrylate) (PEM) in *l*-butanol, a Θ-solvent for both polymers. The overall polymer weight fraction, w_2, was put equal to 0.30 and ratio PMMA/PEMA was taken as 70/30. The extrusion was performed at 85°C. The inside part of the fibrils consists mainly of PMMA, containing domains that contain more of the PEMA. The deposition on the surface of these fibrils is mainly composed of PEMA. A schematic representation of the structure of such a fibre is given in *Figure 3b*. In view of the above discussion on the influence of the experimental conditions on the final morphology of a demixed and vitrified or crystallized system, it is clear that this fibre morphology is also, to a large extent, determined by the experimental conditions mentioned above. Parameters like extrusion rate and cooling rate during this extrusion have to be added to this list. By changing one or several of these parameters, important differences in morphology can be realized[6,7].

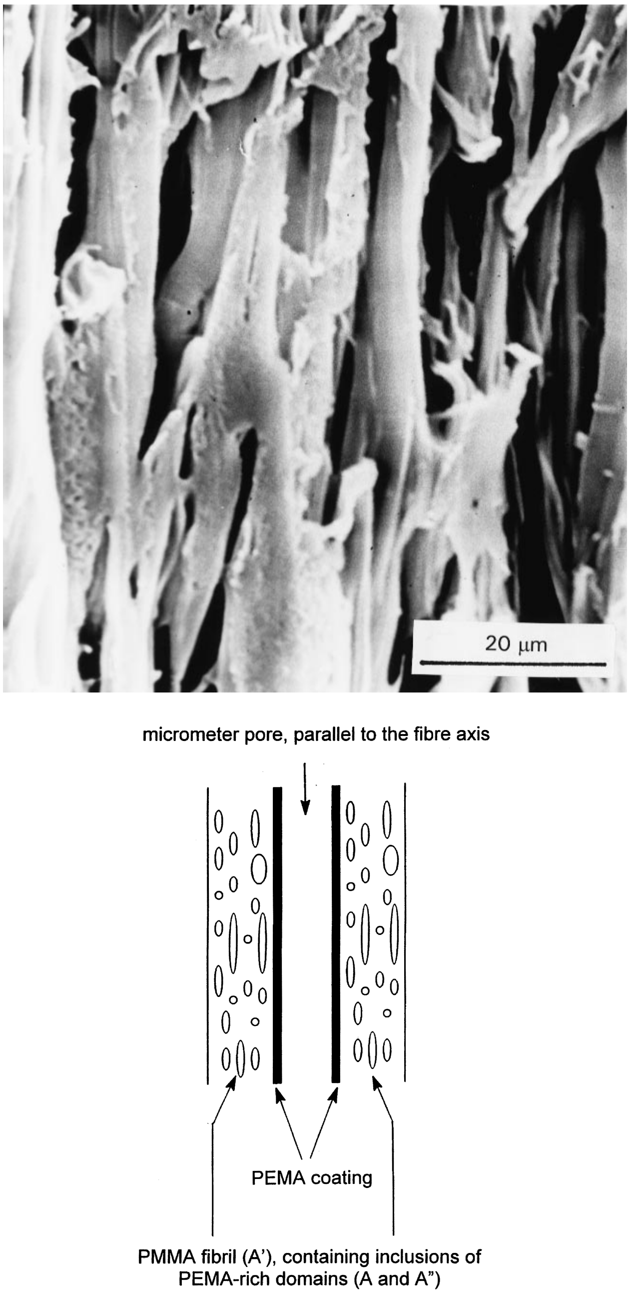

Figure 3 Fibre morphology obtained by extrusion of a solution of PMMA and PEMA in *1*-butanol. Ratio PMMA/PEMA = 70/30; $w_2 = 0.30$

Phase relations leading to this complex fibre formation

This process of complex fibre formation can only be understood through the detailed analysis of the phase behaviour of the three-component system. Such an analysis was already presented in a previous paper for the system PMMA/PEMA/*1*-butanol[10], which also contains the necessary experimental details. The process can be easily transferred to another solvent as long as both polymers show a UCST behaviour in this solvent and by preference an interference between L–L demixing and vitrification above room temperature. An interesting example is the system PMMA/PEMA/*1*-decanol.

Three demixing phenomena have to be considered: polymer–polymer demixing between PMMA and PEMA,

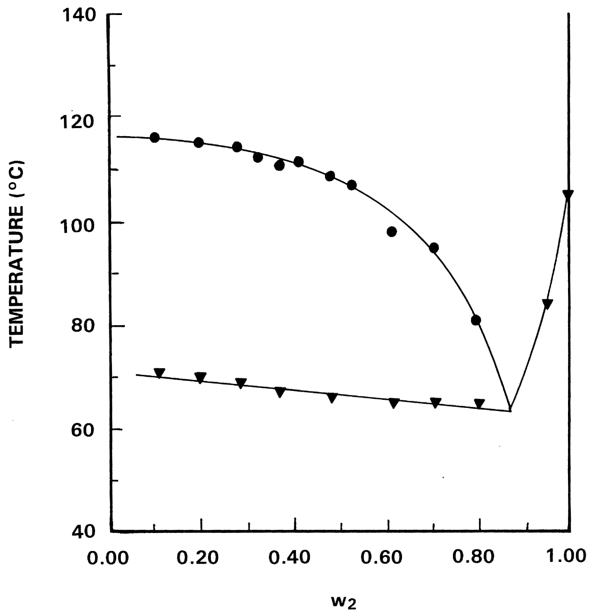

Figure 4 Quasi-binary temperature–concentration diagram of the system PMMA/*1*-decanol. ●, floculation curve; ▼, T_g–concentration

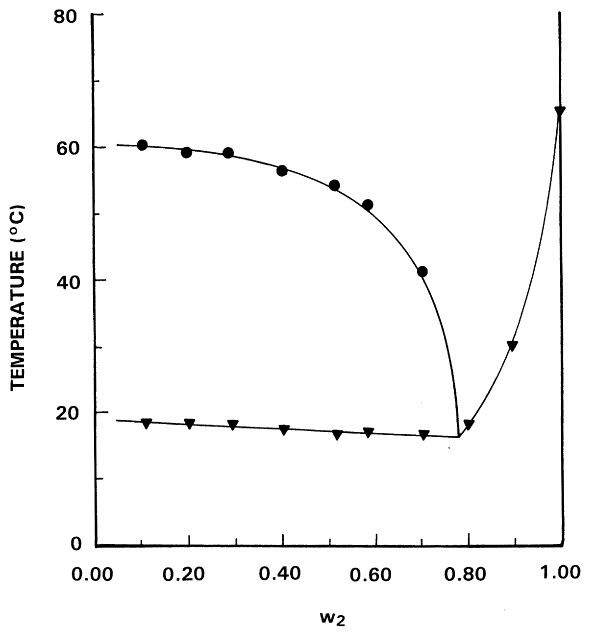

Figure 5 Quasi-binary temperature–concentration diagram of the system PEMA/*1*-decanol. ●, floculation curve; ▼, T_g–concentration

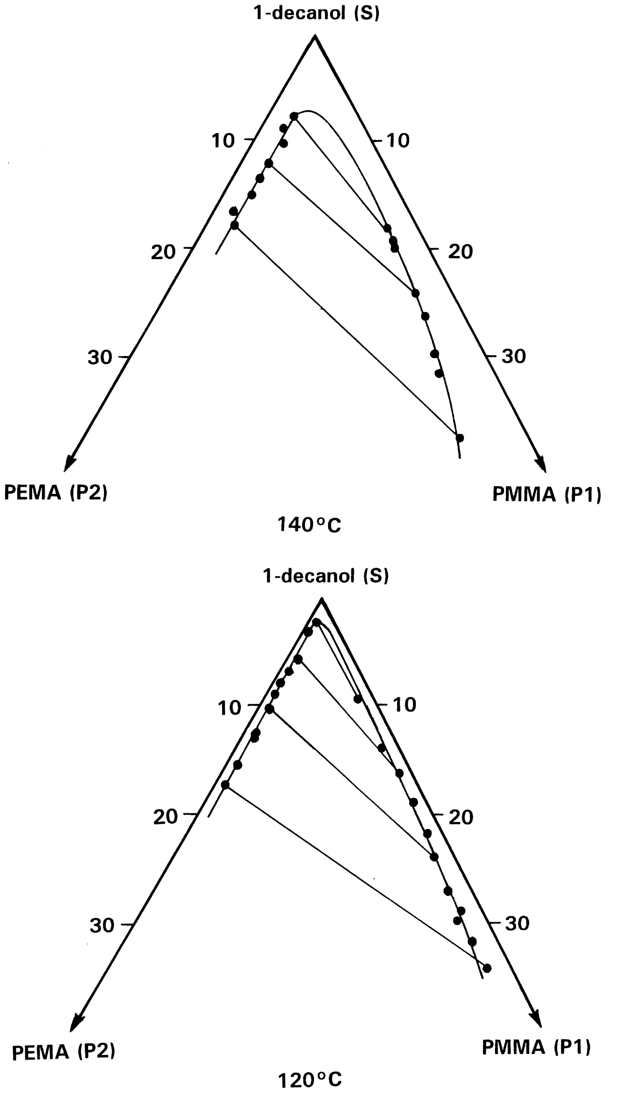

Figure 6 Isothermal composition diagram for PMMA/PEMA/*1*-decanol at two different temperatures: (a) 140; (b) 120°C. ●, coexisting concentrations; (————) tie lines

called PP demixing, in a common solvent, and two polymer–solvent demixing processes in the quasi-binary situations PMMA/*1*-decanol (SP1) and PEMA/*1*-decanol (SP2). These systems are called quasi-binary because of the polydisperse nature of the polymer. These quasi-binary temperature–concentration relations are represented in *Figures 4 and 5*. The floculation points were obtained by optical observations and calorimetric measurements and a floculation curve was drawn by hand through these points (●). The glass transition (T_g) – concentration relation (▼) is also represented in these figures. These data were obtained by calorimetry. In the high concentration region the decrease of T_g with increasing solvent content corresponds to the plastification of the polymer by the solvent. The increase of T_g under the floculation curve with decreasing overall polymer concentration can be ascribed to the molar mass distribution[10]. Polymers with a certain degree of molecular mass distribution have to be treated as multi-component systems and their solutions are not strictly binary. Theoretical considerations of such systems have shown that the concentrations of the coexisting phases that are generated during demixing will be further apart when the overall starting concentration is lower. A decrease of this overall concentration will lead to a decrease of the concentration of the dilute phase and an increase of the concentration of the concentrated phase. As a consequence, the T_g of this concentrated phase will increase with the overall polymer content. It has been shown that T_g becomes non-variant when samples with a narrow molecular mass are used[1,8].

The investigation of the ternary behaviour was subdivided into two parts: PP demixing and SP1 + SP2 demixing. Only PP demixing could be studied optically. Once this demixing has taken place, the system becomes opaque and any further demixing can only be localized by calorimetry.

Typical experimentally obtained sections through the ternary system in the high temperature region above the binary polymer–solvent demixing are represented in *Figure 6a,b* for two different temperatures. The miscibility gap of

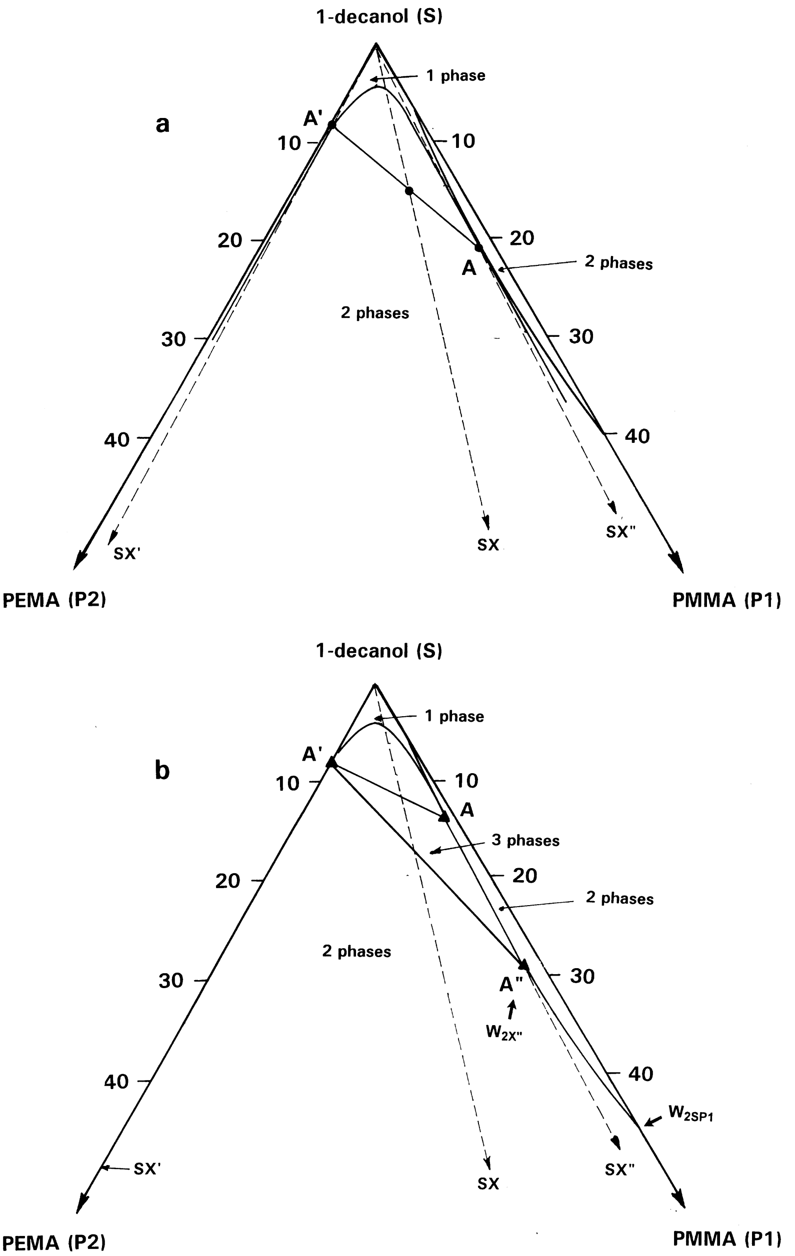

Figure 7 Quasi-ternary phase diagrams for PMMA/PEMA/*1*-decanol. (a) Coalescence of SP and PP gaps by critical point A, coexisting with phase A′. (b) Formation of a three-phase triangle A, A′, A″ by cooling of state (a)

the two polymers in a common poor solvent extends into the composition triangle and nearly reaches the corner representing the solvent. At high temperatures, far above the Θ-temperature of the two quasi binary systems, the system separates into two phases that differ in composition and overall concentration. This phase separation goes to completion within 30 min, even at an overall polymer concentration as high as 30%.

The phases can be separated after quenching in liquid nitrogen and breaking the vitrified system along the interface. Analysis of the constituents then allows plotting of the coexisting phase compositions as shown in *Figure 6*. This temperature dependence demonstrates the UCST character of the process. Cooling below 120°C initiates demixing SP1 and SP2. The maximum separation temperatures are 120°C for SP1 and 63°C for SP2.

The interference of these demixing processes will be discussed on the basis of the schematized equilibrium processes in *Figure 7*. Below 120°C, the miscibility gap in SP1 extends into the composition triangle, as indicated schematically in *Figure 7a*. and eventually touches the PP miscibility gap at A. If the system were strictly ternary, A would represent a critical phase in equilibrium with another liquid phase A′. On further cooling the tie line A–A′ changes into a three-phase triangle A–A′–A″ (*Figure 7b*). Such a classic equilibrium consideration can lead to the description of the different phase transitions that can take place in such a quasi ternary system like a mixture with a ratio P1/P2 = 70/30. Its overall composition is plotted on *SX*, *X* defining the P1/P2 ratio in the mixture. At, e.g. 125°C, PP demixing has taken place and phases A′ and A have formed and *SX*″ represents the composition axis for the P1/P2 mixture in phase A. Similarly for phase A′ we have *SX*′. In order to observe demixing in *SX*″, the temperature must be decreased below 120°C, the maximum separation temperature in SP1. The phase transition would then occur at a lower overall polymer concentration (w_2X) than it does in SP1 ($w_{2\mathrm{SP1}}$). Such a behaviour has been observed and has

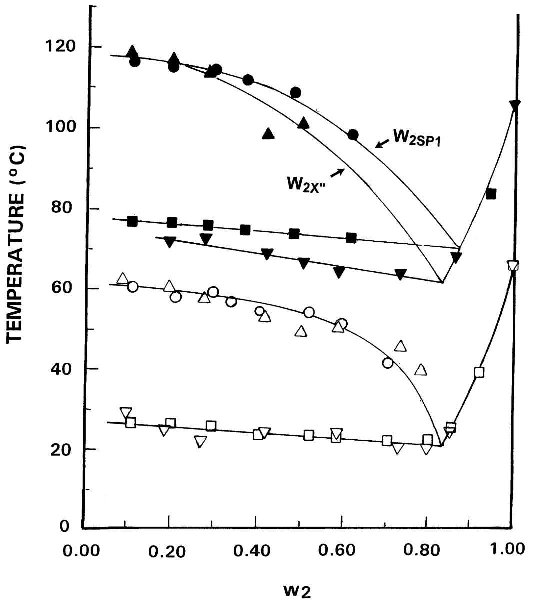

Figure 8 Temperature–concentration diagram of the quasi-binary systems for PMMA/PEMA/*1*-decanol (ratio PMMA/PEMA = 70/30). ●, quasi binary demixing of PMMA; ■, T_g–concentration; ▲, SP1 demixing; ▼, T_g–concentration; ○, quasi binary demixing of PEMA; □, T_g–concentration; △, SP2 demixing; ▽, T_g–concentration

been demonstrated in *Figure 8*, which indicates the temperature dependence of the concentrations $w_{2X''}$ and w_{2SP1}. A similar depression is not found on the SP2 side because of the vitrification of $w_{2X''}$ at 64°C disturbing the equilibrium and because of the near coincidence of *SX'* and SP2. The vitrification of the P2 phase in *SX'* sets in at 17°C.

This discussion is only strictly valid under equilibrium conditions. Under practical conditions, especially when one starts from an already demixed situation, an equilibrium, three-phase situation will never be reached. This was deduced from the optical observation of these different transitions when a solution in a test tube is cooled to room temperature.

A solution with $w_2 = 0.07$ is homogeneous at 140°C. At 128°C, a macroscopic phase separation is reached within 30 min. At 119°C, the system will enter the three-phase region, and the corresponding demixing starts in both phases separately. The macroscopic three-phase situation is not yet realized after 30 min, so that further cooling below 63°C will vitrify the P1-rich phase. Cooling to room temperature will induce a SP2 demixing in the upper layer, the P2-rich phase, and vitrification will take place at 17°C. After elimination of the solvent at low temperature, two macroscopic, porous layers will be obtained. One is composed mainly of PMMA with a small inclusion of P2. The top layer will consist mainly of a porous matrix of P2 with some inclusions of P1.

When this demixing and vitrification is combined with an extrusion, porous composite fibres, like the one presented in *Figure 3*, can be obtained. The final morphology will not only depend on the polymer–solvent phase behaviour, but to a large extent on the experimental conditions, as was discussed in Section 1.

POROUS MATERIALS WITH DIFFERENT SUPRAMOLECULAR ORGANIZATION

General considerations

When these demixing and freezing processes are performed with solutions of crystallizable polymers like syndiotactic polystyrene (sPS), porous materials with different levels of supramolecular organization can be obtained. This polymer is capable of adopting different molecular conformations, leading to different crystal modifications[11–32].

Crystallization from the melt or from solution under well-defined conditions of concentration and temperature, leads to the formation of folded-chain, crystalline lamellae in which the polymer chains adopt an all *trans*, planar zigzag or T_4 conformation (α or β-crystal modification)[11–24]. The polymer chains can also adopt a T_2G_2 conformation with the formation of the δ- and γ-modification[13,17,19,20,23]. Clear evidence for the participation of the solvent in the formation of the δ-phase has been presented, while the γ-phase is a solvent-free helix phase. Recently the formation of a mesophase has also been reported[24–26]. The δ-phase is responsible for the formation of almost transparent, elastic gels, even at concentrations as low as $w_2 = 0.001$.

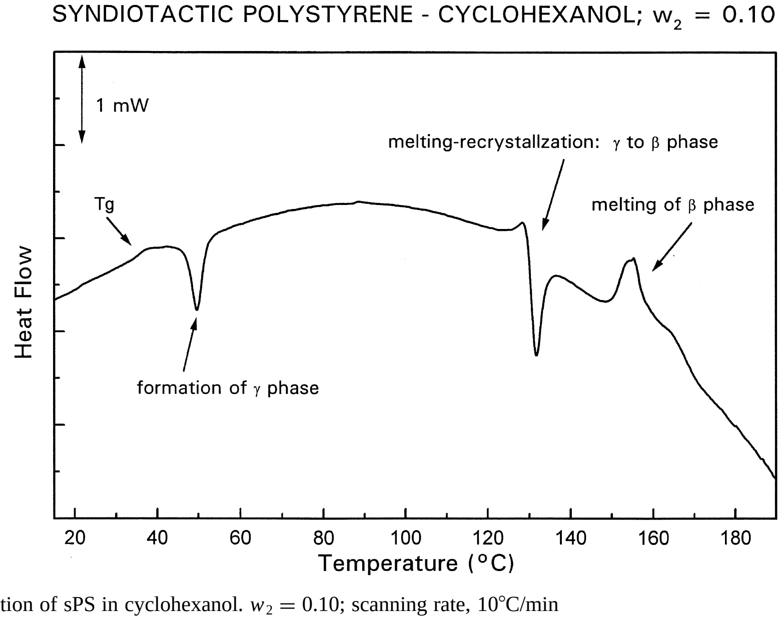

Figure 9 D.s.c. scan of a solution of sPS in cyclohexanol. $w_2 = 0.10$; scanning rate, 10°C/min

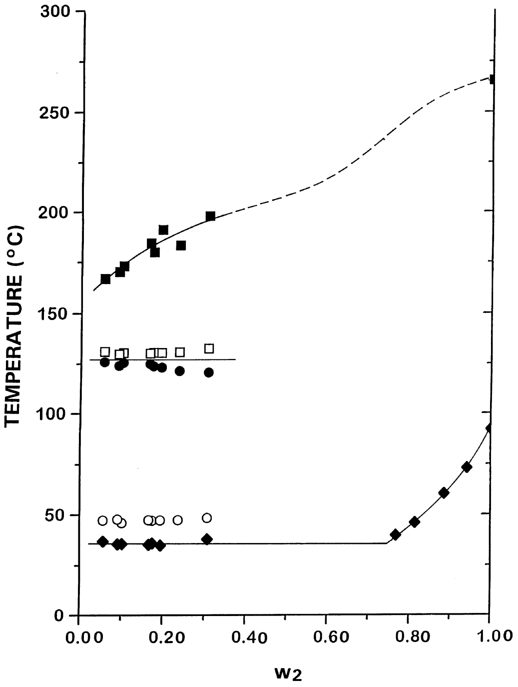

Figure 10 Quasi binary temperature–concentration diagram of the system sPS–cyclohexanol. ■, melting point–concentration relation for the β-phase; □, concentration dependence of the formation of the β-phase; ●, melting of the γ-phase; ○, formation of the γ-phase; ◆, concentration dependence of the glass transition temperature

The study of the temperature–concentration phase behaviour of sPS in different solvents shows that the δ-phase behaves as a polymer–solvent compound[28–33]. Of interest, in view of the production of porous materials, is the behaviour of this system in a Θ-solvent. A detailed analysis of *cis*- and *trans*-decalin has been carried out. In these systems, the β-phase is the stable phase over the whole concentration range, while the invariant incongruent melting of the metastable δ-phase is situated around 125°C[30]. Liquid–liquid demixing, however, was never observed as this demixing proceeds at low temperatures. A Θ-temperature of 12[34] or 10.8°C[35] has been reported for the system [*cis*-decalin/atactic polystyrene] and 20[36] or 23.8°C[35] for the system [*trans*-decalin/atactic polystyrene]. In order to realize this interference between supramolecular structure formation and demixing, a solvent with a much higher Θ-temperature like cyclohexanol has to be used (Θ-temperature for polystyrene is 83°C)[37].

Porous sPS with different types of supramolecular organization

The temperature–concentration relation in the low concentration domain, was constructed by using samples quenched from the isotropic solution at high temperature into liquid nitrogen (wide-angle X-ray scattering (WAXS) or d.s.c.) or ice water (Fourier transform infrared (FT-i.r.)). The differences in quenching procedures were dictated by the experimental setup. A typical d.s.c. scan of a sample with $w_2 = 0.10$ is represented in *Figure 9*. The different phases that are formed during such a temperature scan were characterized by (WAXS) and (FT-i.r.). The different transition temperatures indicated in this graph are plotted as a function of concentration in *Figure 10*. The corresponding WAXS and FT-i.r. observations are reported in *Figures 11 and 12*.

Quenching of a homogeneous solution results in the formation of a demixed, vitrified system which represents a material, composed of domains of almost pure solvent, encapsulated in a membrane-like texture composed of an almost completely amorphous, glassy phase with $w_2 = 0.74$. (*Figure 13a*). This concentration was deduced from the intersection of the invariant T_g–concentration relation below this polymer concentration, with the very pronounced concentration dependence of T_g at higher polymer content. The observation of this invariant T_g over a broad concentration range is the best evidence for the occurrence of this L–L demixing on quenching. This behaviour is different from that reported earlier for PMMA and PEMA. In these systems, the T_g under the demixing curve increases with increasing solvent content. One has, therefore, to conclude that the influence of the polydispersity of the polymer on the composition of the coexisting phase, and therefore on the T_g concentration relation below the demixing line, is strongly dependent on the polymer–solvent system. Direct evidence for the presence of a L–L demixing domain by calorimetric or optical observations could not be obtained from cooling experiments, as the formation of the β-phase interferes with this demixing.

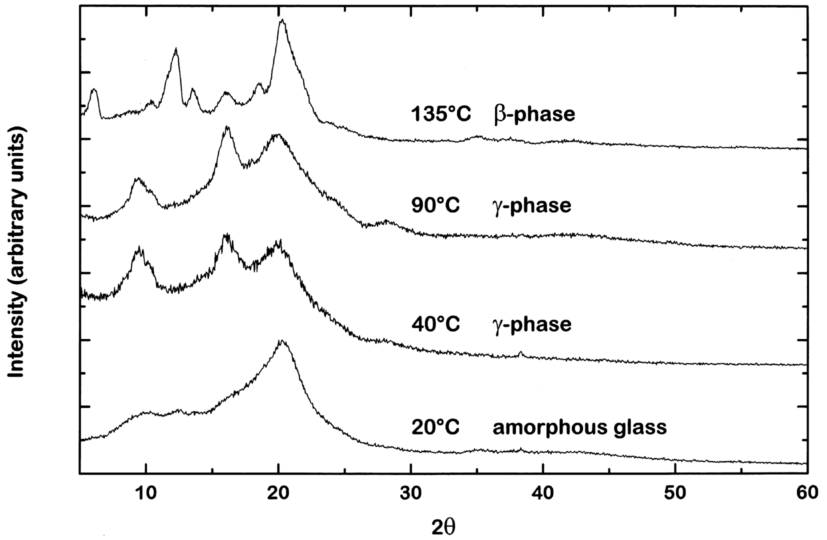

Figure 11 WAXS patterns of the different crystal morphologies of sPS recorded after annealing at the indicated temperatures of samples quenched in liquid nitrogen

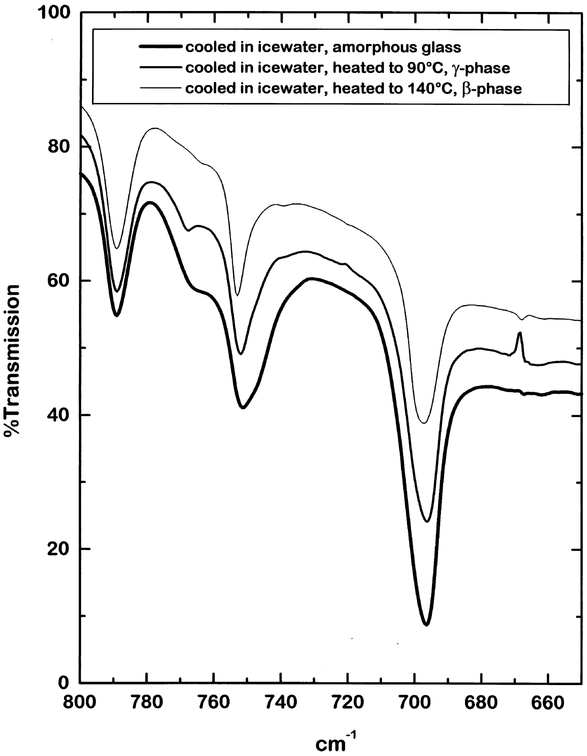

Figure 12 FT-i.r. spectra of the different crystal morphologies of sPS after annealing at the indicated temperatures of samples quenched in ice water

The T_g is followed by exothermic transformation of the glassy domains into the helix phase. This helix phase was clearly identified by WAXS and FT-i.r. observation as the γ-phase (*Figures 11 and 12*). This observation is clearly in contrast with the data obtained in good solvents in which no L–L demixing takes place. In such systems the δ-phase is formed. The formation of the γ-phase instead of the δ-phase when sPS is brought in contact with a Θ-solvent has been reported in the literature[38].

This formation of a supramolecular organization stabilizes the demixed, porous situation so that the system can be heated to a temperature above the remixing temperature (*Figure 13b*). At around 120°C, recrystallization into the β-phase takes place without any destruction of the macroscopic morphology (*Figure 13c*). This morphology deteriorates only at around 140°C when melting of the β-phase sets in.

CONCLUSIONS

Thermally induced phase separation is an interesting method for the preparation of porous materials. This demixing leads in its simplest form, after elimination of the solvent, to the formation of membrane-like structures and by extrusion to porous fibres with oriented microporosity.

The use of two mutual non-compatible polymers in a common Θ-solvent allows the production of composite porous fibres, in which one polymer is coated on the surface of the internal fibrillar structure formed by the second polymer.

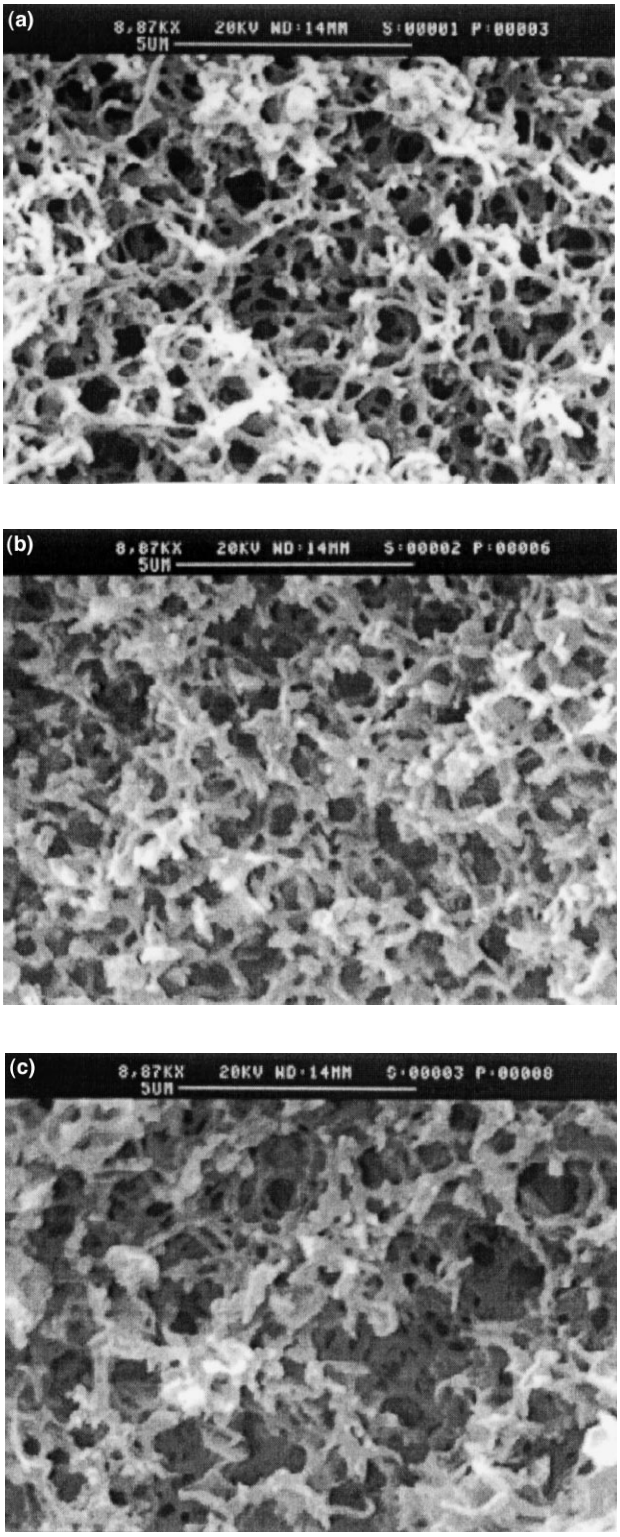

Figure 13 Sampling electron microscope observation of the different porous morphologies of sPS. (a) Room temperature; (b) 90°C; (c) 120°C

With the sPS/cyclohexanol system, porous materials with three different types of supramolecular organization can be realized. The walls of the pores are glassy and almost completely amorphous after quenching, transform on heating in the γ-phase with the molecules in a helix conformation, followed by recrystallization in the β-phase with the molecules in the planar zigzag conformation. In the presence of the solvent, this demixed system can be maintained in its demixed state up to 60°C above the maximum L–L demixing temperature.

ACKNOWLEDGEMENTS

Financial support by the National Fund for Scientific Research, the Interuniversity Poles of Attraction, Belgian

State, Prime Ministers Office, Federal Office for Scientific, Technical and Cultural Affairs (IUAP III/16 and IV-P4/11) are gratefully acknowledged. One of the authors (R.D.C.) wishes to thank the IWONL for a fellowship.

REFERENCES

1. Vanderweerdt, P., Berghmans, H. and Tervoort, Y., *Macromolecules*, 1991, **29**, 3734.
2. Aerts, L., Berghmans, H. and Koningsveld, R., *Makromol. Chem.*, 1993, **194**, 2697.
3. Callister, S., Keller, A. and Hikmet, R.M., *Makromol. Chem., Macromol. Symp.*, 1990, **39**, 19.
4. Arnauts, J. and Berghmans, H., *Polym. Commun.*, 1987, **28**, 66.
5. Arnauts, J. and Berghmans, H., in *Polymer Networks*, chapter 3, ed. W. Burchard and Ross-Murphy. Elsevier Appl. Science, 1990, p. 35.
6. Berghmans, S., Mewis, J., Berghmans, H. and Meijer, H., *Polymer*, 1995, **36**, 3085.
7. Berghmans, S., Berghmans, H. and Meijer, E.H., *J. Membrane Sci.*, 1996, **116**, 171.
8. Vanderweerdt, P., De Cooman, R. and Berghmans, H., *Polym. Commun.*, 1994, **35**, 5141.
9. De Cooman, R., Vanderweerdt, P., Berghmans, H. and Koningsveld, R., *J. Appl. Polym. Sci.*, 1996, **60**, 1127.
10. Koningsveld, R., *Adv. Polym. Sci.*, 1970, **7**, 1.
11. Ishihara, N., Seimiya, T., Kuramoto, M. and Uoi, M., *Macromolecules*, 1986, **19**, 2465.
12. Greis, O., Asano, T., Xu, J. and Petermann, J., *J. Z. Kristallogr.*, 1988, **192**, 58.
13. Immirzi, A., de Candia, F., Inannelli, P. and Zambelli, A., *Makromol. Chem., Rapid Commun.*, 1988, **9**, 761.
14. Shimane, Y., Ishioka, T., Chatani, Y. and Ijitsu, T., *Polym. Prep. Jpn. (Eng. Ed.)*, 1988, **37**, E428.
15. Greis, O., Xu, J., Asano, T. and Petermann, J., *Polymer*, 1989, **30**, 590.
16. Vittoria, V., Russo, R. and de Candia, F., *J. Macromol. Sci., Phys.*, 1989, **B28**, 419.
17. Doherty, D. and Hopfinger, A., *Macromolecules*, 1989, **22**, 2472.
18. Kobayashi, M., Nakaoki, T. and Ishihara, N., *Macromolecules*, 1989, **22**, 4377.
19. Guerra, G., Vitagliano, V., De Rosa, C., Petraccone, V. and Corradini, P., *Macromolecules*, 1990, **23**, 1539.
20. Vittoria, V., Russo, R. and de Candia, F., *Makromol. Chem., Macromol. Symp.*, 1990, **39**, 317.
21. De Rosa, C., Guerra, G., Petraccone, V. and Corradini, P., *Polym. J.*, 1991, **23**, 1435.
22. Rapacciuolo, M., De Rosa, C., Guerra, G., Mensetieri, G., Apicella, A. and Del Nobile, M.A., *J. Mater. Sci. Lett.*, 1991, **10**, 1084.
23. Vittoria, V., Russo, R. and de Candia, F., *Polymer*, 1991, **32**, 18.
24. Chatani, Y., Shimane, Y., Inoue, Y., Inagaki, T., Ishioka, T., Ijitsu, T. and Yukinari, T., *Polymer*, 1992, **33**, 488.
25. Petraccone, V., Auriemma, F., Dal Pogetto, F., De Rosa, C., Guerra, G. and Corradini, P., *Makromol. Chem.*, 1993, **194**, 1335.
26. de Candia, F., Guadagno, G. and Vittoria, V., *J. Macromol. Sci., Phys.*, 1994, **B33**, 347.
27. Manfredi, C., De Rosa, C., Guerra, G., Rapacciuolo, M., Auriemma, F. and Corradini, P., *Macromol. Chem. Phys.*, 1995, **196**, 2795.
28. Chatani, Y., Shimani, Y., Inagaki, T., Ijitsu, T., Yukinari, T. and Shikuma, H., *Polymer*, 1993, **34**, 1620.
29. Deberdt, F. and Berghmans, H., *Polymer*, 1993, **34**, 2192.
30. Deberdt, F. and Berghmans, H., *Polymer*, 1994, **35**, 1964.
31. Roels, T., Deberdt, F. and Berghmans, H., *Macromolecules*, 1994, **27**, 6216.
32. Berghmans, H. and Deberdt, F., *Phil. Trans. R. Soc. London A*, 1994, **348**, 117.
33. Daniel, C., Deluca, M.D., Guenet, J.-M., Brûlet, A. and Menelle, A., *Polymer*, 1996, **37**, 1237.
34. Guenet, J.-M., Lotz, B. and Wittmann, J.-C., *Macromolecules*, 1985, **18**, 420.
35. Kulicke, W.M. and Prescher, M., *Makromol. Chem*, 1984, **185**, 2619.
36. Wolf, B.A. and Jend, R., *Makromol. Chem.*, 1977, **178**, 1811.
37. Reiss, C. and Benoit, T., *J. Polym. Sci. C*, 1968, **16**, 3079.
38. de Candia, F., Romano, G., Russo, R. and Vittoria, V., *Colloid Polym. Sci.*, 1993, **217**, 454.